Advanced Composites and Hybrid Materials (2023) 6:149
https://doi.org/10.1007/s42114-023-00725-1

RESEARCH

Microencapsulated phase change material through cellulose nanofibrils stabilized Pickering emulsion templating

Wei Liu[1] · Qingyi Lin[1] · Siyu Chen[1] · Hongbin Yang[1] · Kun Liu[1] · Bo Pang[2] · Ting Xu[1] · Chuanling Si[1]

Received: 26 May 2023 / Revised: 13 July 2023 / Accepted: 25 July 2023 / Published online: 5 August 2023

Abstract

Phase change materials (PCMs) possess remarkable capability to store and release substantial amounts of energy during the processes of melting and crystallization across a wide temperature range, thus holding great promise in applications related to temperature regulation and thermal energy storage. Herein, to effectively address PCM leakage and enhance thermal conduction, PCM microcapsules with melamine–formaldehyde resin (MF) shell were prepared using in situ polymerization of Pickering emulsions stabilized by cellulose nanofibrils (CNFs). CNFs were selected as the stabilizers for the Pickering emulsions and as reinforcing nanofillers for the MF shell, owing to their excellent emulsifying capability, high mechanical strength, and sustainable nature. Paraffin wax (PW) was utilized as the PCM material. The resulting PCM microcapsules with MF resin shells and PW core had a diameter ranging from 2 to 4 μm. Results showed that microcapsule with the core–shell ratio of 2 (Micro-2.0) exhibited the highest latent heat of crystallization and latent heat of fusion, measuring approximately 128.40 J/g and 120.23 J/g, respectively. The encapsulation efficiency of Micro-2.0 was determined to be approximately 79.84%.

Keywords Cellulose nanofibrils · Phase change materials · Pickering emulsion · Microcapsule

1 Introduction

Energy consumption is expected to increase significantly in the coming decades, because of population and economic growth [1–3]. To date, most energy is still generated by traditional fossil fuels [4, 5]. Therefore, improving energy efficiency and transitioning to green energy sources have become crucial [6–8]. As the most abundant energy source available on the earth, solar energy is a widespread green thermal energy resource and is considered to be the most promising solution to the growing energy crisis [9, 10]. Additionally, it is worth noting that waste heat is a major source of recoverable energy loss. Thermal energy storage is an effective solution to make full use of waste heat and solar thermal energy, offering great possibilities for reducing fossil fuels consumptions, and alleviating energy crisis [11, 12]. Among current thermal energy storage technologies, latent heat energy storage that can provide high-energy densities per unit mass/volume at nearly constant temperatures by changing the phase of a material, usually a phase change material (PCM), has been recognized as one of most promising approaches [13, 14]. Of note, PCM are materials that can absorb or release a significant amount of heat during the phase transition while maintaining a constant temperature [15, 16]. The heat absorbed or released during this phase transition is known as latent heat [17, 18]. PCMs are generally classified into three main categories including organic (e.g., paraffin wax (PW), fatty acids, and esters), inorganic (e.g., salt hydrates, metals, and metal alloys), and eutectic PCMs (e.g., sodium acetate trihydrate and potassium nitrate, or organic compounds like fatty acids combined with alcohols) [19, 20]. Almost these PCMs, organic phase change materials, such as PW and fatty acids, are

✉ Bo Pang
bo.pang@mmk.su.se

✉ Ting Xu
xuting@tust.edu.cn

✉ Chuanling Si
sichli@tust.edu.cn

[1] Tianjin Key Laboratory of Pulp and Paper, Tianjin University of Science and Technology, Tianjin 300457, China

[2] Department of Materials and Environmental Chemistry, Stockholm University, Svante Arrheniusväg 16C, 106 91 Stockholm, Sweden

attractive for latent heat energy storage due to their stable chemical properties, minimal undercooling, wide range of phase transition temperatures, and high heat enthalpy [21, 22]. However, the wide application of organic PCMs still face significant challenges such as volume change during phase transition, leakage, and low thermal conductivity [23, 24]. One solution to these issues is microencapsulation, which involves enclosing the PCM in microcontainers or capsules [25]. Microencapsulation can effectively prevent leakage during phase transition and increase the specific surface area between PCMs and the matrix, thereby improving thermal conductivity [26, 27].

Of note, it is important to ensure that the microcapsules remain stable and uniform over time during the microencapsulation process. To protect phase change materials, polymer shells can be used as encapsulating materials, such as melamine–formaldehyde resin (MF) [28], polyurethane (PU) [29], polystyrene (PS) [30, 31], acrylic resin [32], and poly(methyl methacrylate) (PMMA) [33]. These shells can provide a barrier between the PCM and the surrounding environment, protecting it from external factors that may cause it to degrade or lose its thermal properties [19].

Pickering emulsions, a type of emulsion stabilized by solid particles instead of conventional surfactants, can also be used as a promising platform for incorporating and stabilizing PCMs [34, 35]. The solid particles adsorb at the oil–water interface, forming a physical barrier that prevents the droplets from coalescing [36, 37]. This results in stable emulsions with a long shelf life and increased resistance to shear and coalescence [38]. The use of Pickering emulsions as a platform for PCM stabilization has several advantages over other methods, including improved stability, reduced agglomeration, and increased surface area for heat transfer [39, 40]. Moreover, the physical barrier formed by the interfacial solid particles can effectively prevent PCM leakage [41, 42]. The solid particles used to stabilize Pickering emulsions can be a wide range of materials including silica, metal oxides, clays, and cellulose nanomaterials [43, 44].

Among them, cellulose nanomaterials, for instance, cellulose nanofibers (CNFs), derived from cellulose, have attracted much attention for a wide range of applications including but not limited to those related to Pickering emulsions because of their high specific surface area, easy modification, and good biocompatibility, just to name a few [45–47]. In our previous work, $FeCl_3$-catalyzed formic acid hydrolysis combined with high-pressure homogenization to produce CNFs from industrial kraft pulp was reported [48]. The surface properties of CNFs, especially the surface wettability, can be easily tuned by changing the hydrolysis time. In addition, the obtained CNFs were able to successfully stabilize Pickering emulsions, and the emulsions showed good stability at various ionic strengths from 0 to 1 M NaCl and high temperature of 80 °C.

Herein, as shown in Fig. 1, various PW/MF microcapsules with MF polymer as the shell and PW as the core were fabricated using CNFs-stabilized Pickering emulsions as the template. The chemical components, morphology, thermal storage performance, and thermal reliability of PW/MF microcapsules were comprehensively studied.

2 Materials and methods

2.1 Materials

CNFs suspension with a concentration of around 1 wt% was prepared via $FeCl_3$-catalyzed formic acid hydrolysis in combination with high-pressure homogenization method according to our previous work [48]. Sodium chloride (NaCl) was purchased from Aladdin Reagent (Shanghai) Co.,

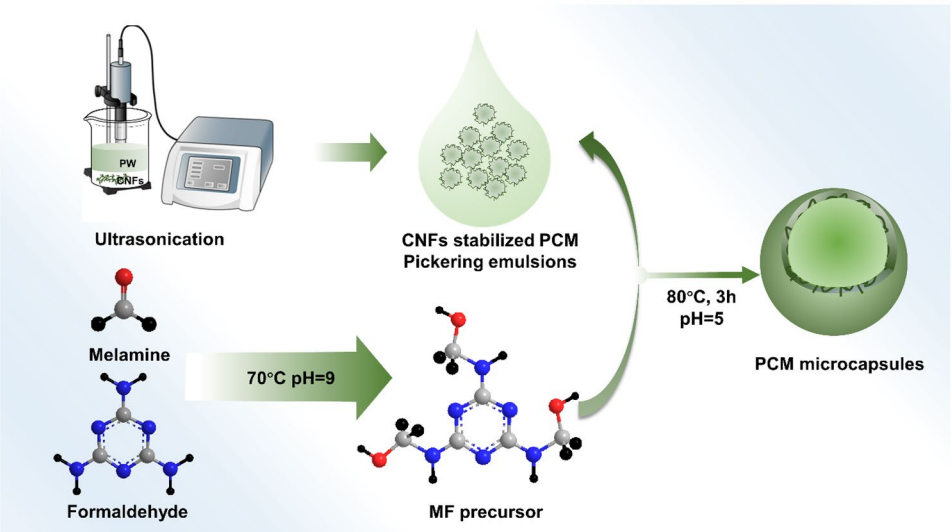

Fig. 1 Schematic illustration of the preparation of PCM microcapsules using CNFs as stabilizers via in situ polymerization method

Ltd. Paraffin wax (Pathological grade, the melting point is 60 ~ 62 °C) and citric acid (CA) were obtained from Maclin Biochemical (Shanghai) Co., Ltd. Formaldehyde solution was provided by Yantai Sanhe Chemical Reagent Factory Co., Ltd. Melamine and Triethanolamine were received from Tianjin Damao Chemical Reagent Factory. All chemicals were used as received without further purification.

2.2 Methods

2.2.1 Preparation of CNCs stabilized Pickering emulsions

To prepare CNFs stabilized Pickering emulsions, 0.5 wt% NaCl (0.08 g) was added to the 10 mg/mL CNFs (8 mL) in order to decrease the repulsion between CNFs. Paraffin (2 g) was added into 8 mL of the CNFs suspension and heated to 80 °C until the paraffin completely melted. The molten mixtures were emulsified by a tip sonicator (FB505, Fisher Scientific, USA) for 10 min (3 s on/2 s off) under the power lever of 60%. After ultrasonication, 10 g of deionized water was added to dilute the emulsion and CA solution (0.5 mol/L) was used to adjust the pH of the emulsion to about 5.

2.3 Preparation of the PCM microcapsules with CNFs and MF hybrid shell

To synthetize MF prepolymer solution, formaldehyde and melamine were sequentially added in a mass ratio of 1:8 into the flask containing 10 mL of the deionized water in order. The mixtures were stirred at 70 °C while adjusting the pH to around 9 with triethanolamine until a clear solution was obtained. After cooling to ambient temperature, the obtained solution was added to the as-prepared CNFs-stabilized PCM Pickering emulsions (10 mL) drop by drop and stirred at 80 °C with a constant stirring speed of 250 rpm. The initial core (paraffin) to shell (MF) ratio varied from 0.5, 1.0, 1.5 to 2.0. The mixtures of the pH were then adjusted to 5 with citric acid solution. After 3 h, the reaction was stopped, and the PCM microcapsules with CNF/MF shell were collected by suction filtering. The wet filter cake was thoroughly washed with 30 wt% ethanol aqueous solution (40 ~ 50 °C) and then dried in the oven for 24 h. The obtained PCM microcapsules were labeled as Micro-0.5, Micro-1.0, Micro-1.5 and Micro-2.0, respectively.

2.3.1 Characterization

The morphology of the Pickering emulsions was observed using an optical microscope (Leica, DM4000 Germany). A MasterSizer® 3000 granulometer (Malvern®, UK) was used to examine the droplet size distribution.

The morphologies of the microcapsule samples were observed by using a scanning electron microscope (JEOL JSM-IT300LV, Japan) at an accelerating voltage of 10.0 kV. A small amount of sample was sprinkled onto conductive tape and sputter coated with gold for 3 ~ 4 times.

The Zeta potential of CNFs suspension was measured using a microscopic electrophoresis device (BTG-Mutek Szp06, Germany). Prior to analysis, the CNFs suspension with a concentration of 0.1 wt% was subjected to ultrasonication at 45 kHz for 10 min. The testing of the CNFs solution was conducted at a pH of 6 and a temperature of 25 °C. To ensure accuracy, all measurements were performed in triplicate, with each measurement consisting of a minimum of 10 runs.

Fourier transform infrared (FTIR) spectra of the samples were recorded using a FTIR-650 spectrometer (Tianjin Gang Dong Sci. and Tech. Development Co., Ltd., China) over the region of 4000 to 400 cm^{-1} with a resolution of 4 cm^{-1}. The powder samples were blended with KBr and compressed into a thin pellet for FTIR examination.

The thermal stabilities of PW, MF shell, and PW/MF microcapsules with CNFs was characterized by a TA Instruments-Waters LLC (USA) at a heating rate of 20 °C/min ranged from room temperature to 600 °C. Three to 5 mg of samples were treated with nitrogen (N_2) atmosphere at a 50 mL/min flow rate.

The thermal properties of PW, MF shell, and PW/MF microcapsules with CNFs were examined by using a differential scanning calorimetry (Netzsch, DSC214 Polyma, Germany), and measured at a heating–cooling rate of ± 10 °C min^{-1} in the temperature range of − 10 ~ 80 °C under the N_2 gas with a flow rate of 50 mL/min. The encapsulation efficiency (η) of PCM microcapsules was calculated according to the following Eq. (1) [49]:

$$\eta = \frac{\Delta H_m + \Delta H_c}{\Delta H_{m0} + \Delta H_{c0}} \times 100\% \quad (1)$$

where the ΔH_{m0} and ΔH_{c0} are the melting and solidifying enthalpies of PW, respectively; ΔH_m and ΔH_c represent the enthalpies of the PCM microcapsules during melting and solidifying, respectively.

3 Results and discussion

In this work, the CNFs employed to stabilize PCM Pickering emulsions were prepared by $FeCl_3$-catalyzed formic acid hydrolysis in combination with high-pressure homogenization method. The resultant CNFs with an average diameter of around 10 nm (Fig. 2a) have a negative zeta potential value of − 20 mV (Fig. 2b). Such nanofibers showed excellent Pickering emulsifying ability because they could be

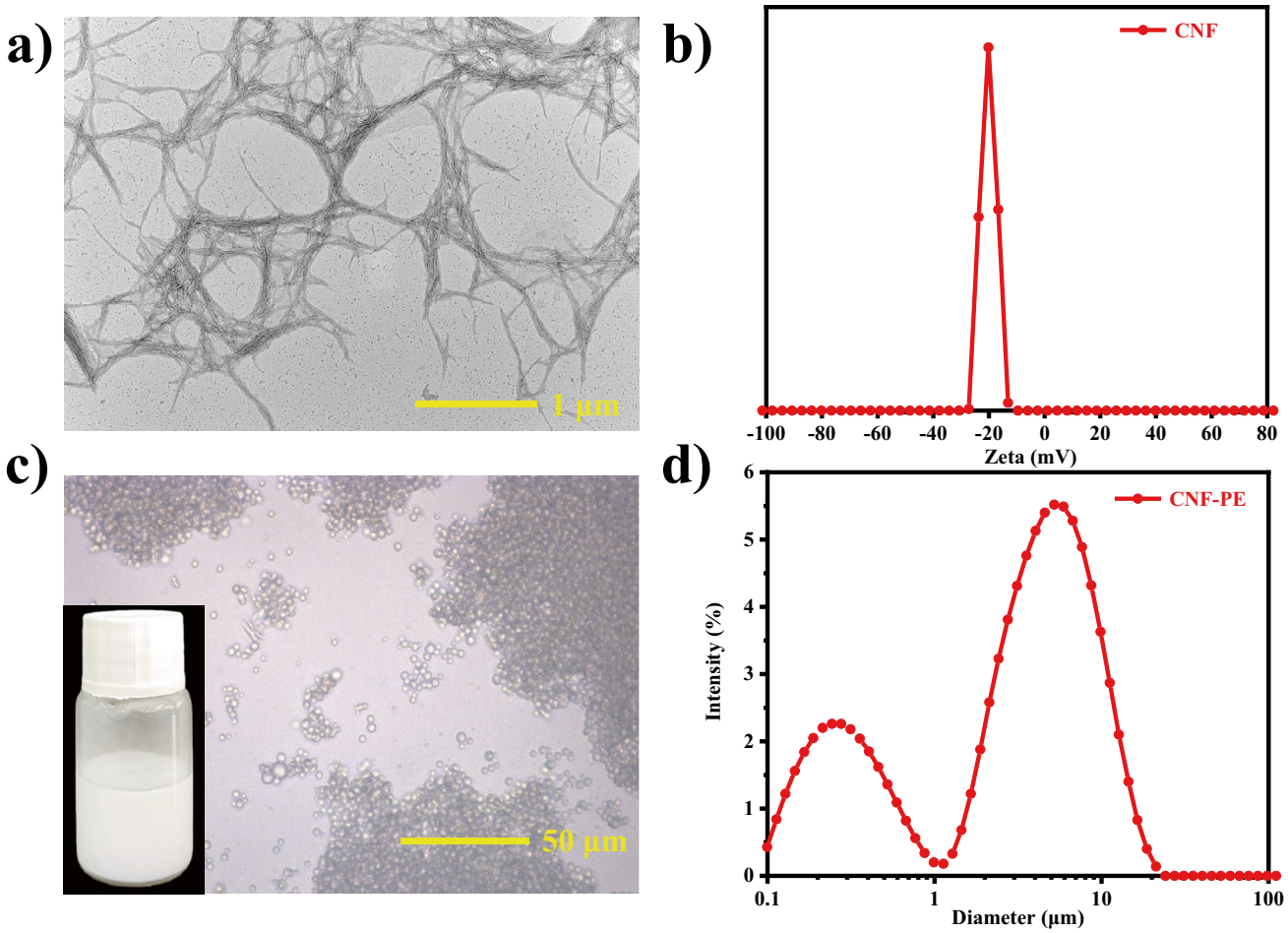

Fig. 2 TEM image (**a**), zeta potential (**b**) of CNFs, optical microscopy images and digital photos (**c**), particle size distribution (**d**) of fresh CNFs stabilized PCM Pickering emulsions

partially wetted by both oil and water phases. Of note, NaCl was added to the CNFs dispersion to lower the electrostatic repulsion between CNFs, thus facilitating the formation of stable Pickering emulsion. Figure 2c shows the optical images of PW Pickering emulsions. Although the emulsion droplets showed slight aggregation, no coalescence was observed. More importantly, even after 3 months of storage at room temperature, no obvious phase separation was observed, indicating the high stability of the CNFs stabilized PW Pickering emulsions. The average diameter of the Pickering emulsions was around 4 μm.

The PCM microcapsules with different core–shell ratios were fabricated via in situ polymerization of MF precursor with CNFs-stabilized PW Pickering emulsions as templates. The formula of PCM microcapsules was listed in Table S1. The size of PCM microcapsules was mainly related to the size of Pickering emulsion droplets, while the core–shell ratio has little effect on it. From Fig. 3, it can be seen that the size of the microcapsules with different core–shell ratios is about 2 ~ 4 μm. PCM microcapsules demonstrated nearly spherical shape with dense MF shell. Compared with other samples, some small indentations were observed in Micro-2.0 (Fig. 3d and h), which may be caused by the volume change of PCM during solidification. CNFs can be clearly observed on the surface of the synthesized microcapsules with MF shells (Fig. 3). It can be found that the microcapsules did not break even under high-vacuum conditions of the SEM, indicating the high mechanical properties of the shells. According to studies previously reported, MF resin incorporated with CNF was expected to have higher mechanical properties than that of pure MF resin. Thus, the microcapsules synthesized in this work are believed to a promising candidate for encapsulating PMs.

The FTIR spectra of the CNFs, PW, MF, and PCM microcapsules are shown in Fig. 4. CNFs show typical vibrations of cellulose at 3397, 2890, 1627, 1438, 1161, 1109, and 886 cm^{-1}, which are associated with the O–H stretching vibration, asymmetric C–H stretching vibration, C–O–H bending, and –O– bending, respectively [50–52]. The peak of CNFs at 1719 cm^{-1} corresponds to the C = O stretching

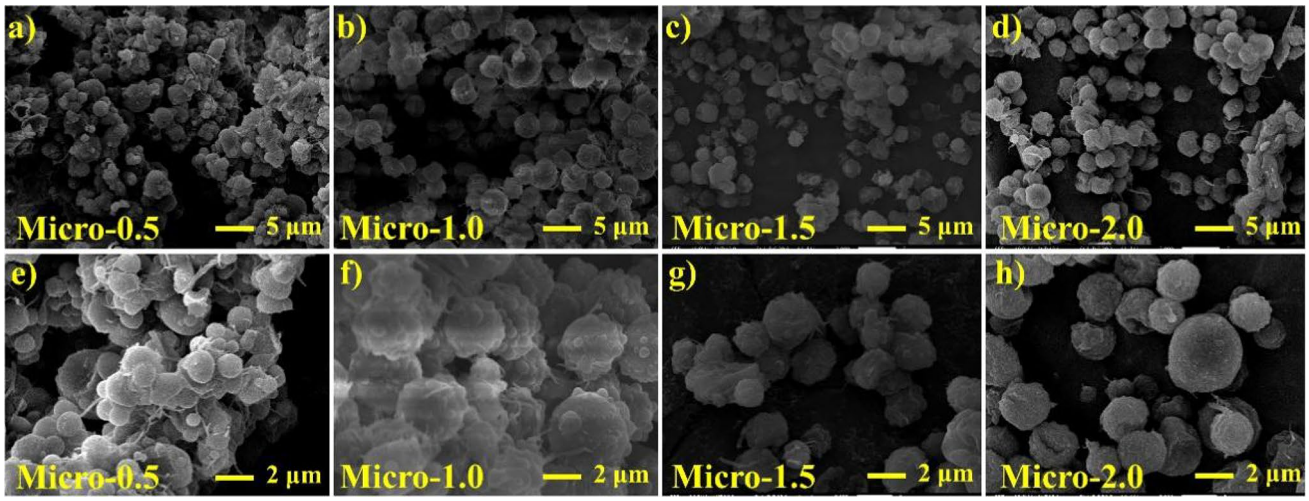

Fig. 3 **a**–**h** SEM images of PCM microcapsules at different magnifications

of ester groups, which is because the fact that FA could react with cellulose through esterification [45, 53]. MF displays vibration at 3410, 1300–1500, 996, and 810 cm^{-1}, which are attributed to the N–H stretching vibrations of a secondary amine, the methylene C–H bending vibration, the C–H out of plane deformations, and bending vibration of triazine ring, respectively [42]. PW shows typical FTIR spectra of alkanes, such as the symmetrical stretching vibration of –CH, $–CH_3$, and $–CH_2$ at 2955, 2915, and 2847 cm^{-1}, deformation vibration of $–CH_2$ and $–CH_3$ at 1461 cm^{-1}, and rocking vibration of $–CH_2$ at 719 cm^{-1} [54]. The PCM microcapsules display the characteristic vibration of PCM, CNFs, and MF, and no new vibration appears, suggesting that there is no chemical reaction between the MF shell and the PCM core materials. The FTIR spectra of the microcapsules contained all the characteristic absorption peaks of the MF shell and the PW core without any other obvious absorption peaks, indicating that the PW had been successfully microencapsulated into the MF shell, and no chemical reaction had occurred between the PW and the MF resin. It is worth note that there is no absorption peak at 1719 cm^{-1} for the microcapsules, which is due to the hydrolysis of the ester groups from the CNFs due to the polymerization under alkaline conditions.

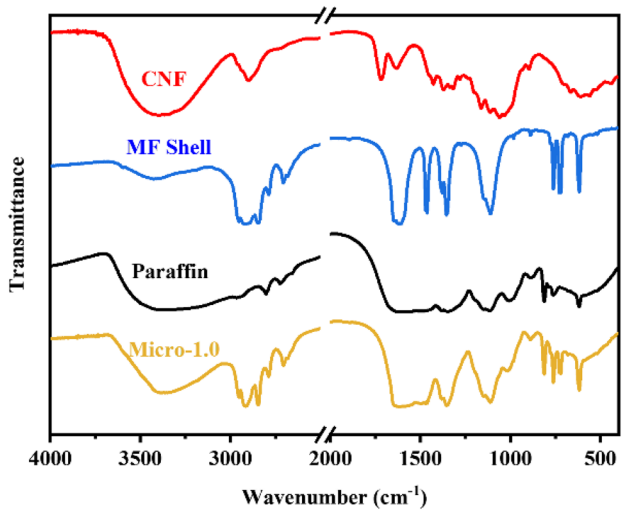

Fig. 4 FTIR spectra of CNFs, MF shell PW, and PCM microcapsule (Micro-1.0)

DSC analyses were conducted to evaluate the phase change properties of the PCM microcapsules including melting and solidifying temperatures, and latent heat storage capacities. The DSC scans of bulk PW, MF shell, and PCM microcapsules are shown in Fig. 5a. During both heating and cooling scans, bulk PW exhibits two distinct phase-change peaks. The first peak, occurring within a lower temperature range, signifies the solid–solid transition from an ordered phase to a more disordered rotator phase. The second peak, observed at higher temperature ranges, corresponds to the solid–liquid melting process [55]. Moreover, no peak was observed in the DSC curve of MF shell, suggesting that all the latent heat of PW/MF microcapsules was from the PW core. The thermal properties of PW and PCM microcapsules are summarized in Table 1. The melting and solidifying temperatures of PW are approximately in the range of 46–72 °C and 63–34 °C, respectively. The latent heat of melting and freezing of bulk PW was measured as 156.54 and 154.87 J/g, respectively. Thermal properties such as encapsulation efficiency and phase transition enthalpy significantly affect the performance and energy storage capacity of PCM microcapsules. The encapsulation efficiency and phase enthalpy of PCM microcapsules gradually increased when the core–shell ratio increased (Table 1). When the core–shell ratio is 2, the crystallization and melting latent heat values of Micro-2.0 are the largest, about 128.40 J/g and 120.23 J/g, respectively. The encapsulation efficiency of Micro-2.0 is about 79.84%.

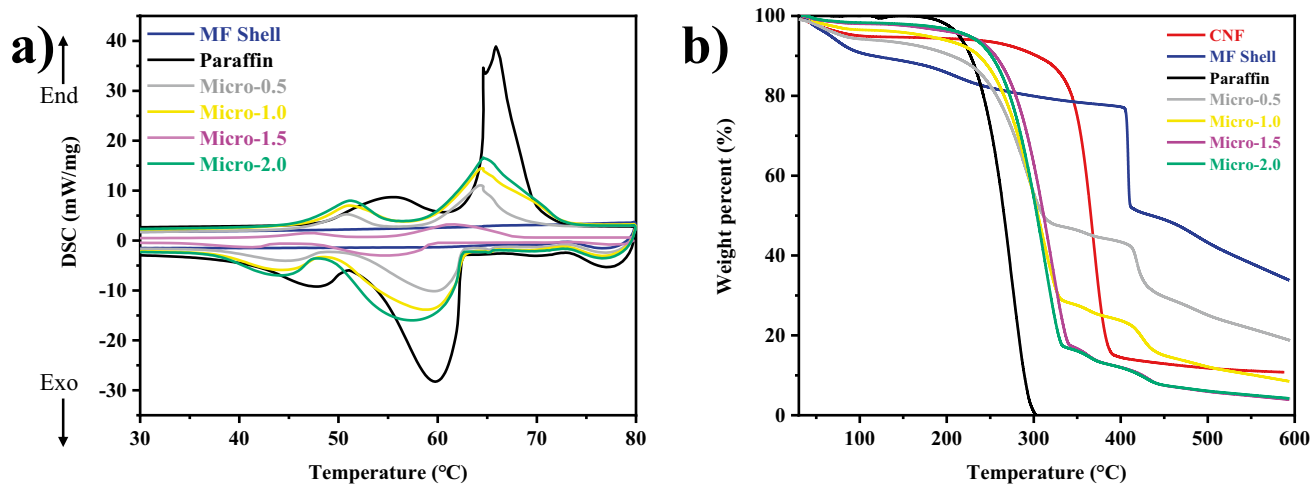

Fig. 5 DSC (**a**) and TGA (**b**) images of PCM microcapsules at different magnifications

Table 1 Phase change properties of PW and PCM microcapsules

Sample	Melting process				Solidifying process				η
	T_{om} (°C)	T_{pm} (°C)	T_{em} (°C)	H_m (J/g)	T_{oc} (°C)	T_{pc} (°C)	T_{ec} (°C)	H_c (J/g)	
PW	48.60	65.56	69.07	156.54	62.37	59.82	41.67	154.87	-
Micro-0.5	46.50	64.44	70.83	66.55	62.43	58.29	38.01	70.10	43.88
Micro-1.0	47.18	64.52	72.40	100.68	62.53	57.88	38.13	105.28	66.14
Micro-1.5	42.45	61.34	67.89	116.6	59.22	54.68	34.79	123.00	76.94
Micro-2.0	46.34	65.07	72.23	120.23	62.47	56.78	37.77	128.40	79.84

T_{oc}, T_{pc}, and T_{ec} onset, peak, and endset temperatures of DSC curve

The thermal properties of microcapsules containing PCM were examined using TGA. Figure 5b illustrates the weight loss and derivative weight loss curves for PCM, MF shell, and PCM microcapsules. PW demonstrates a characteristic weight loss between 180 and 230 °C due to evaporation. The TGA plot reveals that CNFs exhibits a high pyrolysis temperature at approximately 360 °C. Both PW/MF microcapsules exhibit a similar three-step degradation process. In the first step, the thermal degradation of PW primarily contributes to the weight loss of PW/MF microcapsules. The second step occurs between 200 and 340 °C, where the weight loss of the microcapsules aligns precisely with the PW evaporation in this temperature range. Leakage of PW from the microcapsules leads to a rapid increase in internal pressure, causing the fragile MF shell to crack. The third step corresponds to the pyrolysis of the MF shell. Compared to pure PW, the thermal degradation process of microencapsulated PW is significantly delayed, indicating that the MF shell impedes PW volatilization at high temperatures. This phenomenon can be explained by the effective bonding or chemical linking of appropriate CNFs with MF prepolymers, resulting in composite MF shells with enhanced strength against cracking, destruction, and improved thermal stability [56]. Moreover, increasing the core–shell ratio further enhances thermal stability.

4 Conclusions

In summary, PW was successfully microencapsulated using the CNF-stabilized Pickering emulsions as the template. CNFs were employed as Pickering emulsifiers due to their remarkable emulsifying ability, surface functionality, renewability, and biodegradability. The MF shell was formed through the in situ polymerization of MF precursors within the Pickering emulsion resulting in PCM microcapsules with strengthened MF shells reinforced by CNFs. Microcapsules with different core/shell ratios were successfully prepared. Among these microcapsules, Micro-2.0 exhibited the highest latent heat of crystallization and latent heat of fusion, measuring approximately 128.40 J/g and 120.23 J/g, respectively. The encapsulation efficiency of Micro-2.0 was determined to be approximately 79.84%. This work provides a simple yet effective strategy for PCM microencapsulation and could give inspirations for the design of novel thermal energy storage systems.

Author contribution Wei Liu designed the research and wrote the manuscript. Qingyi Lin performed the experiments and data analysis. Siyu Chen sorted the data and figures. Hongbin Yang carried out the data analysis. Kun Liu discussed the results. Bo Pang, Ting Xu, and Chuanling Si supervised the manuscript. All authors have given approval for the final version of the manuscript.

Funding Open access funding provided by Stockholm University. This work was supported by the National Natural Science Foundation of China (32071720, 32271814), Tianjin Excellent Special Commissioner for Agricultural Science and Technology Project (22ZYCGSN00350), and Tianjin Enterprise Technology Commissioner Project (22YDTPJC00930). W. Liu acknowledges the financial support from the China Scholarship Council (No. 202108120056).

Data availability The data that support the findings of this study are available from the corresponding author, Prof. Chuanling Si, upon reasonable request.

Declarations

Conflict of interest The authors declare no competing interests.

References

1. Xu T, Du H, Liu H, Liu W, Zhang X, Si C, Liu P, Zhang K (2021) Advanced nanocellulose-based composites for flexible functional energy storage devices. Adv Mater 33:2101368. https://doi.org/10.1002/adma.202101368
2. Xu T, Liu K, Sheng N, Zhang M, Liu W, Liu H, Dai L, Zhang X, Si C, Du H, Zhang K (2022) Biopolymer-based hydrogel electrolytes for advanced energy storage/conversion devices: properties, applications, and perspectives. Energy Storage Mater 48:244–262. https://doi.org/10.1016/j.ensm.2022.03.0137
3. Liu H, Xu T, Cai C, Liu K, Liu W, Zhang M, Du H, Si C, Zhang K (2022) Multifunctional superelastic, superhydrophilic, and ultralight nanocellulose-based composite carbon aerogels for compressive supercapacitor and strain sensor. Adv Funct Mater 32:2113082. https://doi.org/10.1002/adfm.202113082
4. Liu W, Liu K, Du H, Zheng T, Zhang N, Xu T, Pang B, Zhang X, Si C, Zhang K (2022) Cellulose nanopaper: fabrication, functionalization and applications. Nano-Micro Lett 14:104. https://doi.org/10.1007/s40820-022-00849-x
5. Liu W, Zhang S, Liu K, Yang H, Lin Q, Xu T, Song X, Du H, Bai L, Yao S, Si C (2023) Sustainable preparation of lignocellulosic nanofibrils and cellulose nanopaper from poplar sawdust. J Clean Prod 384:135582. https://doi.org/10.1016/j.jclepro.2022.135582
6. Yang S, Shi C, Qu K, Sun Z, Li H, Xu B, Huang Z, Guo Z (2023) Electrostatic self-assembly cellulose nanofibers/MXene/nickel chains for highly stable and efficient seawater evaporation and purification. Carbon Letters. https://doi.org/10.1007/s42823-023-00540-0
7. Li W, Wang G, Sui W, Xu T, Li Z, Parvez A M, Si C (2022) Facile and scalable preparation of cage-like mesoporous carbon from lignin-based phenolic resin and its application in supercapacitor electrodes. Carbon 196:819–827. https://doi.org/10.1016/j.carbon.2022.05.053
8. Lin Z, Li X, Zhang H, Xu BB, Wasnik P, Li H, Singh MV, Ma Y, Li T, Guo Z (2023) Research progress of MXenes and layered double hydroxides for supercapacitors. Inorganic Chemistry Frontiers. https://doi.org/10.1039/D3QI00819C
9. Duan Y, Yang H, Liu K, Xu T, Chen J, Xie H, Du H, Dai L, Si C (2023) Cellulose nanofibril aerogels reinforcing polymethyl methacrylate with high optical transparency. Adv Compos Hybrid Mater 6:123. https://doi.org/10.1007/s42114-023-00700-w
10. Dash M.K, Jain A, Dhruw L, Giri S, Guo Z, Roymahapatra G (2023) Pyridine-M^{2+} [M = Mg, Ca]: a promising organometallic system for potential hydrogen storage: in silico study. J Indian Chem Soc 100: 101048. https://doi.org/10.1016/j.jics.2023.101048
11. Zhang N, Yuan Y, Cao X, Du Y, Zhang Z, Gui Y (2018) Latent heat thermal energy storage systems with solid–liquid phase change materials: a review. Adv Eng Mater 20:1700753. https://doi.org/10.1002/adem.201700753
12. Riahi A, Shafii MB (2023) Experimental evaluation of a vapor compression cycle integrated with a phase change material storage tank for peak load shaving. Engineered Science 23:870. https://doi.org/10.30919/es8d870
13. Liu H, Xu T, Liu K, Zhang M, Liu W, Li H, Du H, Si C (2021) Lignin-based electrodes for energy storage application. Ind Crops Prod 165:113425. https://doi.org/10.1016/j.indcrop.2021.113425
14. Kuravi S, Trahan J, Goswami DY, Rahman MM, Stefanakos EK (2013) Thermal energy storage technologies and systems for concentrating solar power plants. Prog Energy Combust Sci 39:285–319. https://doi.org/10.1016/j.pecs.2013.02.001
15. Song S, Dong L, Qu Z, Ren J, Xiong C (2014) Microencapsulated capric–stearic acid with silica shell as a novel phase change material for thermal energy storage. Appl Therm Eng 70:546–551. https://doi.org/10.1016/j.applthermaleng.2014.05.067
16. Pielichowska K, Pielichowski K (2014) Phase change materials for thermal energy storage. Prog Mater Sci 65:67–123. https://doi.org/10.1016/j.pmatsci.2014.03.005
17. Liu S, Du H, Liu K, Ma M-G, Kwon Y-E, Si C, Ji X-X, Choi S-E, Zhang X (2021) Flexible and porous Co_3O_4-carbon nanofibers as binder-free electrodes for supercapacitors. Adv Compos Hybrid Mater 4:1367–1383. https://doi.org/10.1007/s42114-021-00344-8
18. Xu T, Song Q, Liu K, Liu H, Pan J, Liu W, Dai L, Zhang M, Wang Y, Si C, Du H, Zhang K (2023) Nanocellulose-assisted construction of multifunctional mxene-based aerogels with engineering biomimetic texture for pressure sensor and compressible electrode. Nano-Micro Lett 15:98. https://doi.org/10.1007/s40820-023-01073-x
19. Giro-Paloma J, Martínez M, Cabeza LF, Fernández AI (2016) Types, methods, techniques, and applications for microencapsulated phase change materials (MPCM): a review. Renew Sustain Energy Rev 53:1059–1075. https://doi.org/10.1016/j.rser.2015.09.040
20. Sharma A, Tyagi VV, Chen CR, Buddhi D (2009) Review on thermal energy storage with phase change materials and applications. Renew Sustain Energy Rev 13:318–345. https://doi.org/10.1016/j.rser.2007.10.005
21. Liu H, Du H, Zheng T, Liu K, Ji X, Xu T, Zhang X, Si C (2021) Cellulose based composite foams and aerogels for advanced energy storage devices. Chem Eng J 426:130817. https://doi.org/10.1016/j.cej.2021.130817
22. Xiang H, An J, Zeng X, Liu X, Li Y, Yang C, Xia X (2020) Preparation and properties of polyurethane rigid foam materials

modified by microencapsulated phase change materials. Polym Compos 41:1662–1672. https://doi.org/10.1002/pc.25487
23. Do T, Ko YG, Chun Y, Choi US (2015) Encapsulation of phase change material with water-absorbable shell for thermal energy storage. ACS Sustainable Chemistry & Engineering 3:2874–2881. https://doi.org/10.1021/acssuschemeng.5b00807
24. Jamekhorshid A, Sadrameli SM, Farid M (2014) A review of microencapsulation methods of phase change materials (PCMs) as a thermal energy storage (TES) medium. Renew Sustain Energy Rev 31:531–542. https://doi.org/10.1016/j.rser.2013.12.033
25. Fang G, Chen Z, Li H (2010) Synthesis and properties of microencapsulated paraffin composites with SiO_2 shell as thermal energy storage materials. Chem Eng J 163:154–159. https://doi.org/10.1016/j.cej.2010.07.054
26. Liu C, Rao Z, Zhao J, Huo Y, Li Y (2015) Review on nanoencapsulated phase change materials: preparation, characterization and heat transfer enhancement. Nano Energy 13:814–826. https://doi.org/10.1016/j.nanoen.2015.02.016
27. Ruan J, Chang Z, Rong H, Alomar TS, Zhu D, AlMasoud N, Liao Y, Zhao R, Zhao X, Li Y, Xu BB (2023) High-conductivity nickel shells encapsulated wood-derived porous carbon for improved electromagnetic interference shielding. Carbon 213: 118208. https://doi.org/10.1016/j.carbon.2023.118208
28. Khan A, Ubaid F, Fayyad EM, Ahmad Z, Shakoor RA, Montemor MF, Kahraman R, Mansour S, Hassan MK, Hasan A, Abdullah AM (2019) Synthesis and properties of polyelectrolyte multilayered microcapsules reinforced smart coatings. J Mater Sci 54:12079–12094. https://doi.org/10.1007/s10853-019-03761-9
29. Ma Y, Chu X, Tang G, Yao Y (2013) The effect of different soft segments on the formation and properties of binary core microencapsulated phase change materials with polyurea/polyurethane double shell. J Colloid Interface Sci 392:407–414. https://doi.org/10.1016/j.jcis.2012.10.052
30. Zhang B, Zhang Z, Kapar S, Ataeian P, da Silva BJ, Berry R, Zhao W, Zhou G, Tam KC (2019) Microencapsulation of phase change materials with polystyrene/cellulose nanocrystal hybrid shell via Pickering emulsion polymerization. ACS Sustainable Chemistry & Engineering 7:17756–17767. https://doi.org/10.1021/acssuschemeng.9b04134
31. Gao F, Liu Y, Jiao C, El-Bahy SM, Shao Q, El-Bahy ZM, Li H, Wasnik P, Algadi H, Xu BB, Wang N, Yuan Y, Guo Z (2023) Fluorine-phosphate copolymerization waterborne acrylic resin coating with enhanced anticorrosive performance. J Polym Sci. https://doi.org/10.1002/pol.20230108
32. Meng X, Li Y, AlMasoud N, Wang W, Alomar TS, Li J, Ye X, Algadi H, Seok I, Li H, Xu BB (2023) Compatibilizing and toughening blends of recycled acrylonitrile-butadiene-styrene/recycled high impact polystyrene blends via styrene-butadiene-glycidyl methacrylate terpolymer. Polymer 272:125856. https://doi.org/10.1016/j.polymer.2023.125856
33. Chen Z-H, Yu F, Zeng X-R, Zhang Z-G (2012) Preparation, characterization and thermal properties of nanocapsules containing phase change material n-dodecanol by miniemulsion polymerization with polymerizable emulsifier. Appl Energy 91:7–12. https://doi.org/10.1016/j.apenergy.2011.08.041
34. Dong Z, Liu Z, Shi J, Tang H, Xiang X, Huang F, Zheng M (2019) Carbon nanoparticle-stabilized Pickering emulsion as a sustainable and high-performance interfacial catalysis platform for enzymatic esterification/transesterification. ACS Sustainable Chemistry & Engineering 7:7619–7629. https://doi.org/10.1021/acssuschemeng.8b05908
35. Shah BR, Li Y, Jin W, An Y, He L, Li Z, Xu W, Li B (2016) Preparation and optimization of Pickering emulsion stabilized by chitosan-tripolyphosphate nanoparticles for curcumin encapsulation. Food Hydrocolloids 52:369–377. https://doi.org/10.1016/j.foodhyd.2015.07.015
36. Jia Y, Zheng M, Xu Q, Zhong C (2019) Rheological behaviors of Pickering emulsions stabilized by TEMPO-oxidized bacterial cellulose. Carbohyd Polym 215:263–271. https://doi.org/10.1016/j.carbpol.2019.03.073
37. Meirelles AAD, Costa ALR, Cunha RL (2020) Cellulose nanocrystals from ultrasound process stabilizing O/W Pickering emulsion. Int J Biol Macromol 158:75–84. https://doi.org/10.1016/j.ijbiomac.2020.04.185
38. Pang B, Zhang H, Schilling M, Liu H, Wang X, Rehfeldt F, Zhang K (2020) High-internal-phase Pickering emulsions stabilized by polymeric dialdehyde cellulose-based nanoparticles. ACS Sustainable Chemistry & Engineering 8:7371–7379. https://doi.org/10.1021/acssuschemeng.0c01116
39. Bai L, Xiang W, Huan S, Rojas OJ (2018) Formulation and stabilization of concentrated edible oil-in-water emulsions based on electrostatic complexes of a food-grade cationic surfactant (ethyl lauroyl arginate) and cellulose nanocrystals. Biomacromol 19:1674–1685. https://doi.org/10.1021/acs.biomac.8b00233
40. Chen QH, Liu TX, Tang CH (2019) Tuning the stability and microstructure of fine Pickering emulsions stabilized by cellulose nanocrystals. Ind Crops Prod 141:111733. https://doi.org/10.1016/j.indcrop.2019.111733
41. Zhang Z, Cheng M, Gabriel MS, Teixeira Neto ÂA, da Silva BJ, Berry R, Tam KC (2019) Polymeric hollow microcapsules (PHM) via cellulose nanocrystal stabilized Pickering emulsion polymerization. J Colloid Interface Sci 555:489–497. https://doi.org/10.1016/j.jcis.2019.07.107
42. Zhang Z, Zhang Z, Chang T, Wang J, Wang X and Zhou G (2022) Phase change material microcapsules with melamine resin shell via cellulose nanocrystal stabilized Pickering emulsion in-situ polymerization. Chem Eng J 428. https://doi.org/10.1016/j.cej.2021.131164
43. Li DD, Jiang JZ, Cai C (2020) Palladium nanoparticles anchored on amphiphilic Janus-type cellulose nanocrystals for Pickering interfacial catalysis. Chem Commun (Camb) 56:9396–9399. https://doi.org/10.1039/d0cc03892j
44. Wang H, Gao Z, Wang X, Wei R, Zhang J, Shi F (2019) Precise regulation of the selectivity of supported nano-Pd catalysts using polysiloxane coatings with tunable surface wettability. Chem Commun 55:8305–8308. https://doi.org/10.1039/C9CC03800K
45. Zhang M, Du H, Liu K, Nie S, Xu T, Zhang X, Si C (2021) Fabrication and applications of cellulose-based nanogenerators. Adv Compos Hybrid Mater 4:865–884. https://doi.org/10.1007/s42114-021-00312-2
46. Zhang X, Liu Y, Wang Y, Luo X, Li Y, Li B, Wang J, Liu S (2019) Surface modification of cellulose nanofibrils with protein nanoparticles for enhancing the stabilization of O/W pickering emulsions. Food Hydrocoll 97. https://doi.org/10.1016/j.foodhyd.2019.105180
47. Yokota S, Kamada K, Sugiyama A, Kondo T (2019) Pickering emulsion stabilization by using amphiphilic cellulose nanofibrils prepared by aqueous counter collision. Carbohydr Polym 226:115293. https://doi.org/10.1016/j.carbpol.2019.115293
48. Liu W, Liu K, Wang Y, Lin Q, Liu J, Du H, Pang B, Si C (2022) Sustainable production of cellulose nanofibrils from kraft pulp for the stabilization of oil-in-water Pickering emulsions. Ind Crops Prod 185. https://doi.org/10.1016/j.indcrop.2022.115123
49. Huang Y, Stonehouse A, Abeykoon C (2023) Encapsulation methods for phase change materials – a critical review. Int J Heat Mass Transf 200:123458. https://doi.org/10.1016/j.ijheatmasstransfer.2022.123458
50. Liu K, Liu W, Li W, Duan Y, Zhou K, Zhang S, Ni S, Xu T, Du H, Si C (2022) Strong and highly conductive cellulose nanofibril/silver nanowires nanopaper for high performance electromagnetic interference shielding. Adv Compos Hybrid Mater 5:1078–1089. https://doi.org/10.1007/s42114-022-00425-2

51. Xu T, Wang Y, Liu K, Zhao Q, Liang Q, Zhang M, Si C (2023) Ultralight MXene/carbon nanotube composite aerogel for high-performance flexible supercapacitor. Adv Compos Hybrid Mater 6:108. https://doi.org/10.1007/s42114-023-00675-8
52. Liu H, Xu T, Liang Q, Zhao Q, Zhao D, Si C (2022) Compressible cellulose nanofibrils/reduced graphene oxide composite carbon aerogel for solid-state supercapacitor. Adv Compos Hybrid Mater 5:1168–1179. https://doi.org/10.1007/s42114-022-00427-0
53. Liu K, Du H, Liu W, Zhang M, Wang Y, Liu H, Zhang X, Xu T, Si C (2022) Strong, flexible, and highly conductive cellulose nanofibril/PEDOT:PSS/MXene nanocomposite films for efficient electromagnetic interference shielding. Nanoscale 14:14902–14912. https://doi.org/10.1039/D2NR00468B
54. Zhou J, Xu W, Wang Y, Shi B (2017) Preparation of polyurea microcapsules containing phase change materials in a rotating packed bed. RSC Adv 7:21196–21204. https://doi.org/10.1039/C7RA01805C
55. Zhang Q, Zhao Y, Feng J (2013) Systematic investigation on shape stability of high-efficiency SEBS/paraffin form-stable phase change materials. Sol Energy Mater Sol Cells 118:54–60. https://doi.org/10.1016/j.solmat.2013.07.035
56. Yoo Y, Martinez C, Youngblood JP (2017) Synthesis and characterization of microencapsulated phase change materials with poly(urea−urethane) shells containing cellulose nanocrystals. ACS Appl Mater Interfaces 9:31763–31776. https://doi.org/10.1021/acsami.7b06970